Published in final edited form as:
Magn Reson Imaging. 2010 May ; 28(4): 537–545. doi:10.1016/j.mri.2009.12.006.

On the Measurement of Multi-component T2 Relaxation in Cartilage by MR Spectroscopy and Imaging

ShaoKuan Zheng, PhD and **Yang Xia, PhD***
Department of Physics and Center for Biomedical Research, Oakland University, Rochester, MI 48309

Abstract

The multi-component T_2 relaxation in bovine nasal cartilage (BNC) was investigated by NMR spectroscopy using the CPMG sequence and microscopic MRI (μMRI) method using a CPMG-SE imaging sequence. All experimental data were analyzed by the non-negative least square (NNLS) procedure. Only one T_2 component was found in BNC by both experimental methods (about 113 ms and 170 ms before and after being enzymatically digested by trypsin). Several experimental and specimen-related factors were investigated in this study and it was found that some of them could produce artificial multi-component T_2, including the use of the standard MSME imaging sequence at certain imaging gradients.

Keywords

Multi-component; T_2; bovine nasal cartilage; CPMG; MRI; NNLS

Introduction

Most biological tissues are known to contain multiple pools of water molecules, each representing a sub-population of water in the tissue residing in a particular molecular environment. The studies of multi-component T_2 relaxation in biological tissues are important because each T_2 component has the potential to characterize the mobility and anisotropy [1–6] of a sub-population of water and its exchange with the other water populations in the tissue. In the NMR spectroscopic and imaging studies of cartilage, several reports have documented multi-component T_2 in articular cartilage (AC, which has three well-structured sub-tissue zones) and bovine nasal cartilage (BNC, which is regarded as relatively randomly organized). For example, Reiter et al recently found that native BNC samples contained either three T_2 components (2.3 ms (6.2%), 25.2 ms (14.5%) and 96.3 ms (79.3%)) by NMR spectroscopy method [7], or two T_2 components (7 ms (76%) and 65 ms (24%)) by MRI method [8]. In addition, Keinan-Adamsky et al noticed that the deep part of adult swine articular cartilage had two age-dependent T_2 components (e.g., 12 ms (39%) and 45 ms (61%) for the 12-month old tissue) by the imaging method [9]. Results from these studies show inconsistencies regarding the existence of multicomponent T_2 in both BNC and AC. For example, if there were indeed three T_2 components in BNC, then the multi-

*Corresponding Address: Yang Xia, Ph. D., Department of Physics, Oakland University, Rochester, Michigan 48309, USA, Phone: (248) 370-3420, Fax: (248) 370-3408, xia@oakland.edu.

component T_2 in AC should not be limited only to its deep zone but its entire depth, including the transitional zone. This expectation is due to the similarity between the random molecular architecture of BNC and that in the transitional zone of AC.

Our recent study [10] showed that the bovine nasal cartilage had only one T_2 component if peak intensities less than 2% of the total intensity were ignored, to eliminate the dependence of the data fitting on the experimental noise, by both MR spectroscopy and microscopic MRI (μMRI) methods. In addition, we also found [10] that the canine articular cartilage had only one T_2 component for the entire tissue depth from the superficial zone to the deep zone, if the μMRI voxel size was as fine as 6.76×10^{-4} mm^3 (26-μm transverse resolution and 1-mm slice thickness). This result of 'single-component T_2 in articular cartilage' is qualitatively similar to the NMR spectroscopy work by Henkelman et al [5], who demonstrated that the bulk T_2 relaxation in bovine articular cartilage had at least two peaks centered around 20 and 55 ms at 0°, and that the 20-ms peak largely disappeared when the tissue's orientation was about 55° to the magnetic field. We attribute the appearance of a multi-component T_2 in articular cartilage in the NMR spectroscopy experiment to the co-existence of the multi-zone structure of the bulk tissue [11].

This project was motivated by a desire to investigate these discrepancies. Bovine nasal cartilage was used as the test specimen in this investigation. This is because, in comparison with articular cartilage that has multiple zone structure [11], BNC is usually regarded as having a relatively homogeneous/random distribution at both molecular and morphological levels, hence the results won't be strongly dependent upon the specimen location and orientation in the magnetic field. The use of BNC would also facilitate the comparative study of the same specimen by both NMR spectroscopy and imaging methods. All spectroscopic and imaging data in this project were analyzed by the non-negative least square (NNLS) procedure [12–14], which means that the results in this report were obtained without *a priori* assumptions about the number of T_2 components and any initial guess of the final solution. Similar to the approaches in literature [15], Monte Carlo simulations were performed throughout the NNLS procedure to determine the requirement of signal-to-noise ratio (SNR) for multi-component T_2 analysis according to our experimental condition.

Materials and Methods

Samples of Bovine Nasal Cartilage

Bovine nasal cartilage was obtained fresh from a local slaughter house (C. Roy, Inc., Yale, MI). The tissue was immersed in physiological saline (154 mM NaCl in deionized water) and stored at −20 °C before the experiment. Five individual specimens, each about $1.5\times1.5\times8$ mm^3 in size, were harvested from the central part of a large BNC block for the μMRI experiments. After the MRI experiments, these specimens were trimmed to about 1-mm long for the NMR spectroscopy experiments (since the slice thickness in imaging experiment was 1 mm). Another three specimens from a nearby location were digested using an enzymatic trypsin protocol overnight. The detailed digestion protocol can be found elsewhere [16], where about 80% of the proteoglycans in cartilage were expected to be removed. Several other specimens from a nearby location on the same tissue block were also used for different experiments in this report (see the text).

NMR Spectroscopy and Microscopic MRI (μMRI)

NMR spectroscopic and μMRI experiments were performed at room temperature on a Bruker AVANCE II 300 NMR spectrometer equipped with a 7-Tesla/89-mm vertical-bore superconducting magnet and micro-imaging accessory (Bruker Instrument, Billerica, MA). A homemade 4-mm solenoid coil was used for both the imaging and spectroscopy

experiment. For μMRI experiments, the 8-mm-long BNC samples were soaked in saline with 1% protease inhibitor (Sigma, Missouri) in a 3-mm NMR tube. For NMR spectroscopic experiments, the 1-mm-long BNC specimens were first surface-blotted dry and then immersed in Fluorinert FC-77 liquid (3M Co., St. Paul, MN), which has low water solubility and similar susceptibility to tissue, to minimize the influence of the magnetic susceptibility difference between the tissue and air [17,18]. The first order automatic shimming provided by Bruker Co. was performed before any spectroscopy and imaging experiment (unless noted otherwise).

NMR spectroscopic measurements of bulk T_2 relaxation were performed using a standard CPMG pulse sequence, with the acquisition parameters closely following the protocol by Henkelman et al [5]. A total of 10,000 echoes were acquired (which yielded 5000 data points because only the even echoes were used) and an echo time of 1 ms was used to avoid the spin-locking effect [19]. The 90° rf excitation pulse had a duration of about 3.775 μs; the repetition time (TR) was 12 s; the number of dummy scans was 8; the number of scan was 128 and a minimum SNR of about 2000 was achieved for all experiments.

Quantitative μMRI T_2 experiments were performed using a CPMG magnetization-prepared spin echo imaging sequence [10] (termed as the CPMG-SE in this report) as well as a standard MSME pulse sequence (Multi-Slice-Multi-Echo, only one slice was used in this report) from Bruker Co. As discussed previously [6,10,20], the magnetization-prepared imaging sequence has two well-separated time segments: a leading T_2-weighting segment that contains no gradient pulses and a subsequent imaging segment where all timings are kept constant during the T_2-weighting, hence capable of determining T_2 unambiguously. The 2D imaging parameters were: the field of view (FOV) was 3.2×3.2 mm^2; the imaging matrix size was 32×32; the spectral bandwidth was 100 kHz corresponding to a readout sampling dwell time of 10 μs; the excitation and refocusing pulses were 0.8-ms and 0.507-ms hermite shape pulses, respectively; the slice thickness was 1 mm; the repeat time was 1.8 s; the number of scans was 16. With these imaging parameters, an echo time of 3 ms in the imaging segment and a SNR of about 750 were achieved. For comparison, a standard MSME experiment was also performed for each BNC tissue using the identical imaging parameters, except for the following (unless noted otherwise): the number of images (or the number of echoes) was 120; the repeat time was 3.0 s; the number of averages was 512 and a SNR of about 6000 was achieved. In both CPMG SE and MSME pulse sequences, a pair of crusher gradients in the read direction, which straddled the refocusing RF pulse, was used. These read crushers are variable, depending upon the FOV in the experiment. The MSME sequence also included a pair of crusher gradient in the slice selection axis, which had a constant duration and amplitude of 300 ms and 2.93 Gauss/mm respectively in all imaging experiments.

The echo spacing in the T_2-weighting CPMG segment of the CPMG-SE sequence in μMRI was 1 ms, which was the same as that used in the NMR spectroscopy experiments. The leading contrast segment in CPMG-SE μMRI had 64 even numbered echoes, approximately uniformly spaced on a logarithmic scale over the interval of 2 to 1010 ms: 25 echoes from 2 ms to 50 ms at an interval of 2 ms, 10 echoes from 54 ms to 90 ms at an interval of 4 ms, 10 echoes from 110 ms to 190 ms at an interval of 10 ms, 5 echoes from 210 ms to 290 ms at an interval of 20 ms, 4 echoes from 320 ms to 410 ms at an interval of 30 ms, 7 echoes from 460 ms to 760 ms at an interval of 50 ms, 3 echoes from 810 ms to 1010 ms at an interval of 100 ms. The purpose of using this set of varying echo spacings in the CPMG contrast segment in CPMG-SE μMRI was to capture the information about both the fast-relaxing component as well as the slow-relaxing component [21–23]. Because the echo time between any two 180° refocusing pulses is kept constant, this type of varying echo spacing CPMG experiment will not introduce an error of non-mono-exponential characteristic, which may

"distort relative amplitudes of a multi-component T_2 distribution or generate multiple T_2 components where they do not exist" [23].

NNLS T2 analysis

The non-negative least square (NNLS) procedures [12–14] were implemented using the MatLab codes (MathWorks, Natick, MA) and carried out to analyze the data from both CPMG spectroscopy and imaging experiments. The echo intensities from imaging experiments were the average intensity of each imaging. The signal intensities as a function of the echo time in both CPMG spectroscopy and MRI methods can be written as:

$$y(t_i)=\sum_{j=1}^{M} S_j e^{-t_i/T_{2j}}+C, \quad i=1,2,\ldots,\mathrm{N} \tag{1}$$

where N is the number of echoes, t_i is the i^{th} echo time, $y(t_i)$ is the signal intensity of the i^{th} echo, M is the number of T_2 components, S_j is the intensity of the j^{th} T_2 component, and C is a constant accounting for any offset of the signal. For both simulation and experimental data, 200 (M=200) T_2j values were used, on a logarithmic scale over the interval of 1 to 1000 ms. One additional T_2 value, which was set to infinity, was added to simulate the constant item in Eq. (1). A "least-square based constraint" rule [15] was used to obtain a smooth T_2 distribution. The value of the regularization in the calculation was chosen in such a way that the standard deviation of χ^2 is 101% of the unregularized least square misfit for the experimental data, and that the estimated distribution of T_2 is similar to that of the known T_2 for simulation data. For each T_2 spectrum from the NNLS calculation, any T_2 component with an intensity below a specific threshold (peak area less than 3% of the total area) or with the T_2 value at the peak position lower or higher than a threshold (1.5 ms and 250 ms, respectively) was ignored to eliminate the dependence of the fit on the experimental noise [15,24,25] and the free water component which was not part of the tissue. The NNLS procedure used in this project means that the results in this report were acquired without *a priori* assumptions about the number of T_2 components and any initial guess of the solution.

Simulation of T2 data

Simulation of T_2 data closely followed the procedures previously reported in the literature [7,15,26]. Because the optimal echo time in the CPMG spectroscopy experiment for a given N has been documented extensively [7,15], only the simulation of the admissibility versus SNR was performed according to our specific experimental condition, which means that 64 echoes with the same echo numbers in our imaging experiment were used in the simulation. Three groups of simulation were performed, shown in Table 1, according to the number of T_2 components and the relative weight of each component reported in the literature [7,9,10]. The equation by Graham et al [15] was used to generate the simulated T_2 decay data where each T_2 component was assumed to follow a Gaussian distribution with a 10% standard deviation of each mean T_2 value. A Gaussian random noise was also included to simulate the experimental noise. The statistical admissibility, which is defined as the "percentage of distributions with the correct number of components" [15], was determined by 200 calculation trials for each set of experimental conditions. The analysis criteria for admissibility closely followed the same literature. Estimated components below a specific T_2 threshold (1.5 ms) and a weight value (3%) were ignored.

Results

Admissibility in Multi-T2 Calculation

Fig 1 shows the NNLS analysis results of the admissibility versus SNR for three different component conditions (Table 1), where the T_2 values were selected to approximate our specimen conditions and those reported in the literature [7,9,10]. It is clear that the SNR requirement for a 90%-admissibility is (1) different for different situations, highest for the situation of three T_2 components and lowest for the situation of one T_2 component, and (2) also different for the situations of one T_2 component having different T_2 values. Fig 1 also shows that the SNR dependency of the admissibility can be influenced by the NNLS calculation criteria. For example, without the rule of 'components below specific T_2 threshold (1.5 ms) were ignored' in the NNLS procedure, the SNR requirement for the one T_2 component of 5 ms at the same admissibility increases significantly (open circles vs. solid circles), but this rule has no significant effect on the calculation result of one T_2 component of 50 ms or 150 ms. The signal decay for short T_2 components is more susceptible to the presence of random noise and the influence of any short-T_2 exclusion rule. These calculations further demonstrate that the optimum experimental condition (echo time, echo number, SNR etc.) needs to be selected carefully for each particular experiment [7,15].

T2 Relaxation in Bovine Nasal Cartilage (BNC)

The normalized proton signals from a representative BNC sample (before and after being digested by trypsin) are shown in Fig 2, where Fig 2a and 2b are the results by the CPMG spectroscopy and the CPMG-SE imaging methods respectively. Since the decaying signals are plotted on a logarithmic scale, any deviation from a straight line might imply a second component. As one can see from Fig 2, the signal decays were clearly single exponential, by both spectroscopic and imaging methods. This observation of single exponential decay was confirmed by the NNLS analysis, shown in Fig 3 as the single peak. The trypsin treatment of the BNC specimens increases the T_2 relaxation time of the tissue by about 50%, reflecting the increased amount of free water in the tissue following the removal of the proteoglycan macromolecules by the enzymatic method [16]. The T_2 results of BNC from both NMR spectroscopy and imaging methods were summarized in Table 2, which also includes the results of two T_2 components by the MRI MSME method.

Note that some minor 'components' could occasionally show up in the T_2 plots by the NNLS method, such as the 1-ms peak in Fig 3a and about 10-ms peak in Fig 3b. Because these 'minor components' were small (less than 3% in population weight) and not consistent (either absent or having a variable value between 1 ms and 20 ms in this group of BNC specimens), these peaks were attributed to the influence of experimental noise, instrument instability or sample inhomogeneity (for example, accidental squeezing and, hence, re-compartment of waters during the preparation of the sample).

The Influence of the Imaging Parameters on Multi-T2 Measurement

To test the reliability of the imaging measurement of multi-component T_2 by MRI, a series of experiments were performed by using different imaging protocols and by changing the strength of the imaging gradients. Fig 4 shows the T_2 results from the same specimen when the standard MSME imaging sequence was used at different matrix sizes and FOVs. When the FOV was 6.4×6.4 mm^2 (the solid line in Fig 4) or 12.8×12.8 mm^2 (data not shown), the T_2 results from the MSME method were the same as that from the CPMG-SE method – only one T_2 component was found in the BNC specimen. However, when a reduced FOV of 3.2×3.2 mm^2 (hence stronger imaging gradients) was used, two T_2 components could be found in the same BNC specimen. In addition to the extra T_2 components at the stronger gradients, one can also notice that the T_2 value of the main peak of the specimen decreases

when the imaging gradient is getting stronger, from ~ 100 ms at 12.8×12.8 mm^2 FOV (data not shown), to ~ 85 ms at 6.4×6.4 mm^2 FOV (solid lines in Fig 4), to ~ 45–55 ms at 3.2×3.2 mm^2 FOV (Fig 4).

The Influence of the Experimental Imperfections on Multi-T2 Measurement

To test the potential influence of sample size on the T_2 measurement (which is related to the homogeneity of B_0 and B_1 and also probably the sample heterogeneity), a set of CPMG spectroscopic experiments was carried out by changing the length of the specimens. Given that the length of our rf coil was 8 mm, we started with a 10-mm-long sample and then trimmed it to 5-mm-long, both being longer than our normal CPMG spectroscopy sample (about 1-mm-long, the same size of our imaging slice). Both samples were immersed in the susceptibility-matching FC-77 liquid. No consistent multi-component T_2 was found (the 5-mm result is shown in Fig 5 as the solid line, and the minor peak at 33 ms is only 2.53%).

To test the influence of the magnetic susceptibility on the multi-T_2 measurement, the above 5-mm-long BNC specimen was measured twice, with and without the FC-77 liquid, in NMR spectroscopy. The T_2 results are shown in Fig 5. While the specimen immersed in FC-77 liquid has only one T_2 component, the specimen without FC-77 liquid (i.e., specimen exposed to air in an NMR tube) has two major T_2 components. The T_2 value of the main peak of the tissue was reduced by about 10% due to the influence of the magnetic susceptibility difference between the specimen and air. The second T_2 peak for the exposed specimen was centered at 270 ms, which was caused by the water condensation on the glass tube (confirmed visually after the experiment).

To further test the influence of the experimental parameters on the multi-T_2 measurement, two deliberate alterations were carried out during the CPMG spectroscopic experiments: (1) changing the durations of the 90° and 180° pulse times (Fig 6a) (using the specimens about 1-mm-long and in FC-77 liquid) and (2) reducing the homogeneity of the magnetic field manually or using the 1-mm-long specimen without the susceptibility-matching FC-77 liquid (Fig 6b). By changing the duration of the hard pulses by up to ±50%, T_2 in BNC was surprisingly still a single component (Fig 6a), although some minor peaks did appear in the NNLS analysis, sometimes up to about 4% of the total population. However, these minor components were not consistent during the repeated experiments. (Fig 6a only shows the results by increasing the 90° pulse time from the calibrated value of 3.775 μs. We also reduced the pulse time by up to 50% and obtained essentially the same results.) By reducing the homogeneity of the magnetic field (or using a 1-mm-long specimen without the FC-77 liquid, which resulted in a wide spectroscopic line width because of the magnetic susceptibility difference between tissue and air), one could distort the line-shape of the T_2 decay, as shown in Fig 6b when the spectroscopic line width was increased deliberately to four times the normal line width (by changing the shim values).

Discussion

Multi-component T_2 relaxation can be used to characterize the complex chemical, physical and morphological environment in biological tissues. However, an accurate measurement of multi-component T_2 in tissue is not trivial – it can be influenced by many factors, experimental and specimen-related. Among the experimental factors, it is well known that a long train of 180° refocusing pulses in the CPMG experiment is sensitive to the system errors from the imperfection of RF pulse and static field inhomogeneity [27–29]. Furthermore, a very short echo time could result in the increase of the measured T_2 due to the spin locking effect [19,30]. In addition, a long echo time could result in an error from diffusion effect when an inhomogeneous field is present. Among the specimen-related factors, the anisotropy of the macromolecules in the specimen, and the induced field

inhomogeneity from the magnetic susceptibility discontinuities between the specimen and environment can also manipulate the T_2 measurement [5,20,31]. When the structure in the tissue is not homogenous (such as the zonal structure in articular cartilage), one has no choice but to incorporate the imaging method into the experimental protocol – often via the multi-echo approach [32–40].

In this project, the simulation of T_2 data was performed first to make sure that the experimental SNR is sufficient to distinguish multi-component T_2s in the BNC sample if the multi-component T_2s does exist in the specimen. After this simulation, both NMR spectroscopy and imaging methods were used to measure the T_2 relaxation in the BNC tissue. For the CPMG spectroscopy experiments, small size samples (about $1.5\times1.5\times1$ mm^3) immersed in FC-77 liquid were used to minimize the spatial localization problem in the sample and to improve the homogeneity for both the RF field and static magnetic field over the whole sample.

For the imaging experiments, both MSME (only one slice was used in this project) and CPMG-SE sequences were used to study the same specimens. The results (e.g., Fig 3 and Fig 4) clearly show that the CPMG-SE imaging sequence, although requiring a longer experimental time, is superior to the standard multi-echo sequence (MSME) for the accurate determination of T_2 in ex vivo imaging. The fundamental reason for the superiority of the CPMG-SE sequence is due to its CPMG magnetization-prepared contrast segment [20,41], where the T_2 relaxation is being weighted without the presence of any gradient. In contrast, the different T_2-weightings in the ‘standard’ multi-echo imaging sequence (MSME) involves spatial-encoding gradients and selective 180° pulses, which could result in artifacts [32–40]. The three MSME experiments shown in Fig 4 had the phase-encoding gradient of 11.70, 5.85, 2.93 Gauss/mm respectively and the frequency-encoding gradient of 7.30, 7.30, 3.65 Gauss/mm respectively. The last combination of gradients resulted in a single-component T_2 measurement while the first two gradient combinations both resulted in two-component T_2 for the same specimens. In addition, stronger imaging gradients (i.e., higher resolution) also cause the T_2 values to be shorter (Fig 4).

Based on previously reported results [10] and those from the current study, we can conclude that there is only one T_2 component in bovine nasal cartilage, whether one uses CPMG spectroscopy method or CPMG-SE imaging method. (Though a small T_2 component varied from 1 to 20 ms with a weight less than 3% could occasionally be found, especially for native samples before it was degraded by trypsin.) This conclusion is inconsistent with some reports in the literature [7–9]. Without knowing the full set of experimental details, we can only speculate that these inconsistencies might be caused by previously mentioned experimental or specimen-related factors discussed earlier. For example, we know from the current study that the MSME sequence used previous investigations [8,9] could cause the appearance of multi-T_2 components in BNC at certain gradient strengths.

It is well accepted that there are at least two proton pools in cartilage [6,42–48]: free water and bound water. (A third proton pool that is a part of the macromolecule (i.e. -OH and/or –NH) can in some cases also be taken into account.) The experimental evidence of one T_2 component in both bovine nasal cartilage and articular cartilage means that the exchange between the bound and free waters in cartilage must be fast comparing with the relaxation process [42,45]. In our previous report [10], we found that after articular cartilage was degraded by trypsin, there were no significant changes for T_2 values in the deep zone of the tissue but an approximately 20% increase for T_2 in the transitional zone was seen when articular cartilage was imaged at the 0° orientation in the magnet. This result implies that although ~ 80% GAG were removed from cartilage by trypsin [16], the increased amount of water had no significant effect on the overall T_2 value in the deep zone because the T_2

mechanism in the deep zone of articular cartilage is dominated by the residual dipolar interaction due to its well-organized collagen fibers [49]. In comparison, the same amount of GAG removal can result in a 20% increase of T_2 value in the transition zone of articular cartilage because of its relatively random structure. Hence the water content in cartilage can only have significant influence on the overall T_2 value either when the molecular structure of the tissue is not organized (e.g., BNC and the transitional zone of articular cartilage), or the dipolar interaction is weak (e.g., the collagen fibrils being oriented at the magic angle).

In conclusion, the experiments in this report investigated the distribution of T_2 relaxation in bovine nasal cartilage and found that there was only one T_2 component. Several experimental and specimen-related factors in the measurement of multi-component T_2 have also been investigated. While the standard MSME imaging sequence can cause the tissue to exhibit artificial multiple T_2 components, the CPMG-SE imaging sequence is robust and reliable, because it minimizes the error caused by the spatial-encoding imaging gradients and takes full advantage of the classic CPMG method in the measurement of T_2 relaxation. This CPMG-SE imaging sequence can also overcome possible errors due to local water inhomogeneities (e.g., water condensation on the surface, local dry-out due to improper blot-drying) in the bulk CPMG spectroscopy experiments.

Acknowledgments

Y Xia is grateful to the National Institutes of Health for the R01 grants (AR 045172 and AR 052353). The authors wish to thank Drs Dieter Gross and Klaus Zick (Bruker BioSpin GmbH, Germany) for providing a CPMG spectroscopy pulse sequence, and Miss Carol Searight and Dr Matt Szarko (Dept of Physics, Oakland University) for editorial comments.

References

1. Swift TJ, Fritz OG Jr. A proton spin-echo study of the state of water in frog nerves. Biophys J 1969;9:54–59. [PubMed: 5782895]
2. Hazlewood CF, Chang DC, Nichols BL, Woessner DE. Nuclear magnetic resonance transverse relaxation times of water protons in skeletal muscle. Biophys J 1974;14:583–606. [PubMed: 4853385]
3. Vasilescu V, Katona E, Simplaceanu V, Demco D. Water compartments in the myelinated nerve. III. Pulsed NMR results. Experientia 1978;34:1443–1444. [PubMed: 309823]
4. Belton P, Ratcliffe R. NMR and compartmantation in biological tissues. Progress in NMR Spectroscopy 1985;17:241–279.
5. Henkelman RM, Stanisz GJ, Kim JK, Bronskill MJ. Anisotropy of NMR properties of tissues. Magn Reson Med 1994;32:592–601. [PubMed: 7808260]
6. Xia Y. Relaxation anisotropy in cartilage by NMR microscopy (μMRI) at 14 μm resolution. Magn Reson Med 1998;39:941–949. [PubMed: 9621918]
7. Reiter DA, Lin PC, Fishbein KW, Spencer RG. Multicomponent T2 relaxation analysis in cartilage. Magn Reson Med 2009;61:803–809. [PubMed: 19189393]
8. Reiter, DA.; Lin, PC.; Fishbein, KW.; Spencer, RG. Multicomponent T2 relaxation in bovine nasal cartilage. In Book of abstracts: the 54th Annual Meeting of the Orthopaedic Research Society; San Francisco. 2008. p. 1648
9. Keinan-Adamsky K, Shinar H, Navon G. Multinuclear NMR and MRI studies of the maturation of pig articular cartilage. Magn Reson Med 2006;55:532–540. [PubMed: 16450338]
10. Zheng S, Xia Y. Multi-components of T2 relaxation in ex vivo cartilage and tendon. J Magn Reson 2009;198:188–196. [PubMed: 19269868]
11. Xia Y. Averaged and depth-dependent anisotropy of articular cartilage by microscopic imaging. Semin Arthritis Rheum 2008;37:317–327. [PubMed: 17888496]
12. Lawson, CJ.; Hanson, RJ. Solving Least Squares Problems. New Jersey: Prentice-Hall, Englewood Cliffs; 1974.

13. Whittall KP, MacKay AL. Quantitative interpretation of NMR relaxation data. J Magn Reson 1989;84:134–152.
14. Whittall KP, Bronskill MJ, Heneklman RM. Investigation of analysis techniques for complicated NMR relaxation data. J Magn Reson 1991;95:221–234.
15. Graham SJ, Stanchev PL, Bronskill MJ. Criteria for analysis of multicomponent tissue T2 relaxation data. Magn Reson Med 1996;35:370–378. [PubMed: 8699949]
16. Xia Y, Farquhar T, Burton-Wurster N, Vernier-Singer M, Lust G, Jelinski LW. Self-diffusion monitors degraded cartilage. Arch Biochem Biophys 1995;323:323–328. [PubMed: 7487094]
17. Tsoref L, Shinar H, Seo Y, Eliav U, Navon G. Proton double-quantum filtered MRI--a new method for imaging ordered tissues. Magn Reson Med 1998;40:720–726. [PubMed: 9797155]
18. Webb S, Munro CA, Midha R, Stanisz GJ. Is multicomponent T2 a good measure of myelin content in peripheral nerve? Magn Reson Med 2003;49:638–645. [PubMed: 12652534]
19. Santyr GE, Henkelman RM, Bronskill MJ. Variation in measured transverse relaxation in tissue resulting from spin locking with the CPMG sequence. J Magn Reson 1988;79:28–44.
20. Xia Y, Farquhar T, Burton-Wurster N, Lust G. Origin of cartilage laminae in MRI. J Magn Reson Imaging 1997;7:887–894. [PubMed: 9307916]
21. Shrager RI, Weiss GH, Spencer RG. Optimal time spacings for T2 measurements: monoexponential and biexponential systems. NMR Biomed 1998;11:297–305. [PubMed: 9802472]
22. Skinner MG, Kolind SH, MacKay AL. The effect of varying echo spacing within a multiecho acquisition: better characterization of long T2 components. Magn Reson Imaging 2007;25:840–847. [PubMed: 17418518]
23. Does MD, Gore JC. Complications of nonlinear echo time spacing for measurement of T2. NMR Biomed 2000;13:1–7. [PubMed: 10668048]
24. Oh J, Han ET, Pelletier D, Nelson SJ. Measurement of in vivo multi-component T2 relaxation times for brain tissue using multi-slice T2 prep at 1.5 and 3 T. Magn Reson Imaging 2006;24:33–43. [PubMed: 16410176]
25. Saab G, Thompson T, Marsh G. Multicomponent T2 relaxation of in vivo skeletal muscle. Magn Reson Med 1999;42:150–157. [PubMed: 10398961]
26. Fenrich FR, Beaulieu C, Allen PS. Relaxation times and microstructures. NMR Biomed 2001;14:133–139. [PubMed: 11320538]
27. Vold RL, Vold RR, Simon HE. Errors in measurements of transverse relaxation rates. J Magn Reson 1973;11:283–298.
28. Majumdar S, Orphanoudakis SC, Gmitro A, O'Donnell M, Gore JC. Errors in the measurements of T2 using multiple-echo MRI techniques. I. Effects of radiofrequency pulse imperfections. Magn Reson Med 1986;3:397–417. [PubMed: 3724419]
29. Majumdar S, Orphanoudakis SC, Gmitro A, O'Donnell M, Gore JC. Errors in the measurements of T2 using multiple-echo MRI techniques. II. Effects of static field inhomogeneity. Magn Reson Med 1986;3:562–574. [PubMed: 3747818]
30. Grucker D, Mauss Y, Steibel J, Poulet P, Chambron J. Effect of interpulse delay on NMR transverse relaxation rate of tissues. Magn Reson Imaging 1986;4:441–443.
31. Kurland RJ, Ngo FQ. Effect of induced field inhomogeneity on transverse proton NMR relaxation in tissue water and model systems. Magn Reson Med 1986;3:425–431. [PubMed: 3724421]
32. Maudsley AA. Modified Carr-Purcell-Meiboom-Gill sequence for NMR Fourier imaging applications. J Magn Reson 1986;69:488–491.
33. Majumdar S, Gore JC. Effects of selective pulses on the measurement of T2 and apparent diffusion in multiecho MRI. Magn Reson Med 1987;4:120–128. [PubMed: 3561241]
34. Majumdar S, Gmitro A, Orphanoudakis SC, Reddy D, Gore JC. An estimation and correction scheme for system imperfections in multiple-echo magnetic resonance imaging. Magn Reson Med 1987;4:203–220. [PubMed: 3574056]
35. Crawley AP, Henkelman RM. Errors in T2 estimation using multislice multiple-echo imaging. Magn Reson Med 1987;4:34–47. [PubMed: 3821477]

36. Barker GJ, Mareci TH. Suppression of artifacts in multiple-echo magnetic resonance. J Magn Reson 1989;83:11–28.
37. Neeman M, Freyer JP, Sillerud LO. Pulsed-gradient spin-echo diffusion studies in NMR imaging. Effects of the imaging gradients on the determination of diffusion coefficients. J Magn Reson 1990;90:303–312.
38. Poon CS, Henkelman RM. Practical T2 quantitation for clinical applications. J Magn Reson Imaging 1992;2:541–553. [PubMed: 1392247]
39. Whittall KP, MacKay AL, Graeb DA, Nugent RA, Li DK, Paty DW. In vivo measurement of T2 distributions and water contents in normal human brain. Magn Reson Med 1997;37:34–43. [PubMed: 8978630]
40. Sled JG, Pike GB. Correction for B(1) and B(0) variations in quantitative T2 measurements using MRI. Magn Reson Med 2000;43:589–593. [PubMed: 10748435]
41. Haase A, Brandl M, Kuchenbrod E, Link A. Magnetization-prepared NMR microscopy. J Magn Reson A 1993;105:230–233.
42. Lüsse S, Knauss R, Werner A, Gründer W, Arnold K. Action of compression and cations on the proton and deuterium relaxation in cartilage. Magn Reson Med 1995;33:483–489. [PubMed: 7776878]
43. Adler RS, Swanson SD, Yeung HN. A three-component model for magnetization transfer. Solution by projection-operator technique, and application to cartilage. J Magn Reson B 1996;110:1–8. [PubMed: 8556231]
44. Liepinsh E, Otting G. Proton exchange rates from amino acid side chains--implications for image contrast. Magn Reson Med 1996;35:30–42. [PubMed: 8771020]
45. Gründer W, Wagner M, Werner A. MR-microscopic visualization of anisotropic internal cartilage structures using the magic angle technique. Magn Reson Med 1998;39:376–382. [PubMed: 9498593]
46. Lattanzio PJ, Marshall KW, Damyanovich AZ, Peemoeller H. Macromolecule and water magnetization exchange modeling in articular cartilage. Magn Reson Med 2000;44:840–851. [PubMed: 11108620]
47. Duvvuri U, Goldberg AD, Kranz JK, Hoang L, Reddy R, Wehrli FW, Wand AJ, Englander SW, Leigh JS. Water magnetic relaxation dispersion in biological systems: The contribution of proton exchange and implications for the noninvasive detection of cartilage degradation. Proc Natl Acad Sci U S A 2001;98:12479–12484. [PubMed: 11606754]
48. Mlynarik V, Szomolanyi P, Toffanin R, Vittur F, Trattnig S. Transverse relaxation mechanisms in articular cartilage. J Magn Reson 2004;169:300–307. [PubMed: 15261626]
49. Xia Y. Magic angle effect in MRI of articular cartilage - A review. Invest Radiol 2000;35:602–621. [PubMed: 11041155]

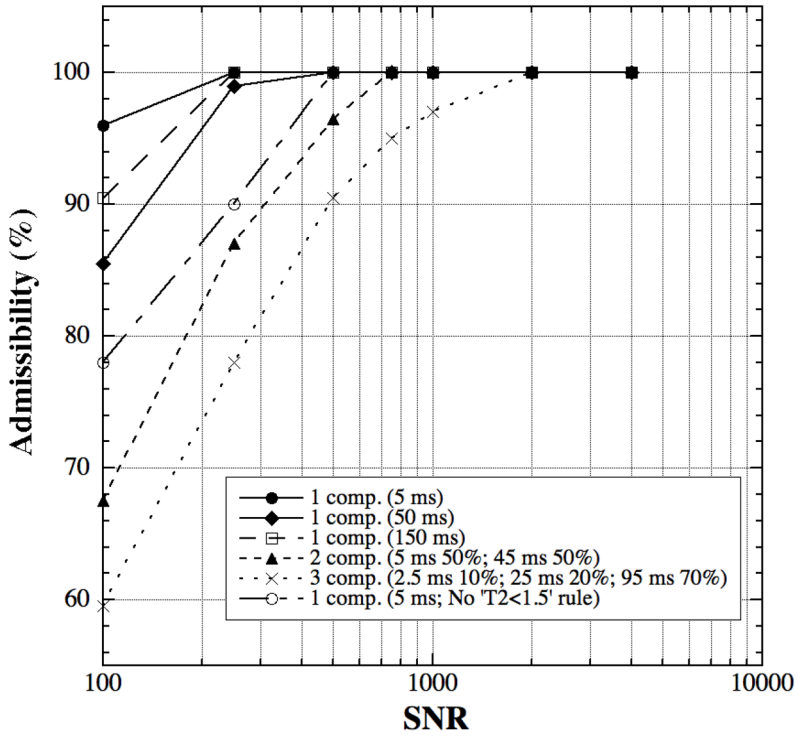

Fig 1.

The admissibility of the simulated T_2 relaxation data when T_2 has one, two, or three components.

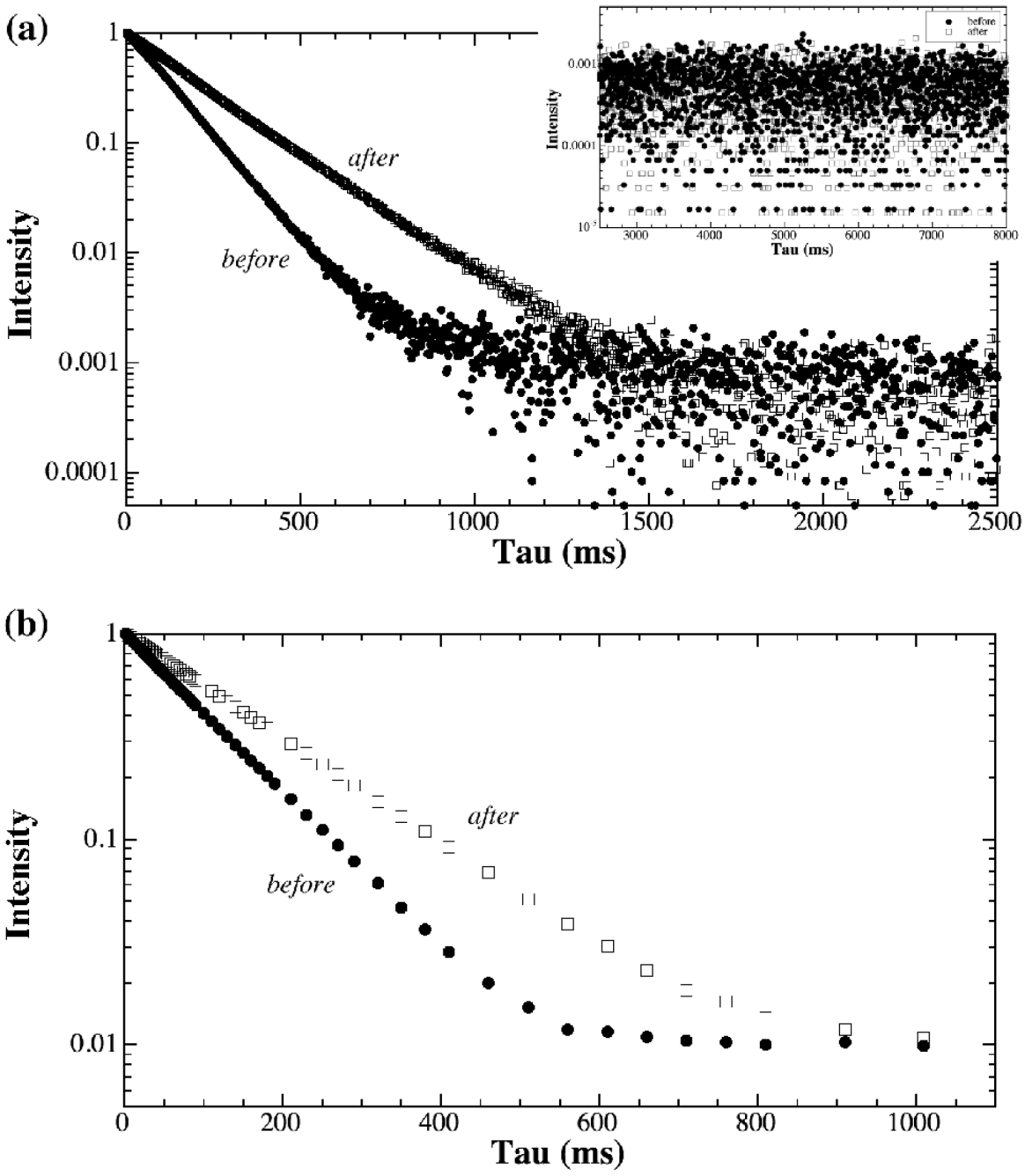

Fig 2.

The signal intensity plots from (a) NMR spectroscopy using the CPMG sequence and (b) μMRI using the CPMG-SE sequence, for bovine nasal cartilage before (solid) and after (open) the trypsin treatment. The insert in (a) shows the tail section of the signal decay.

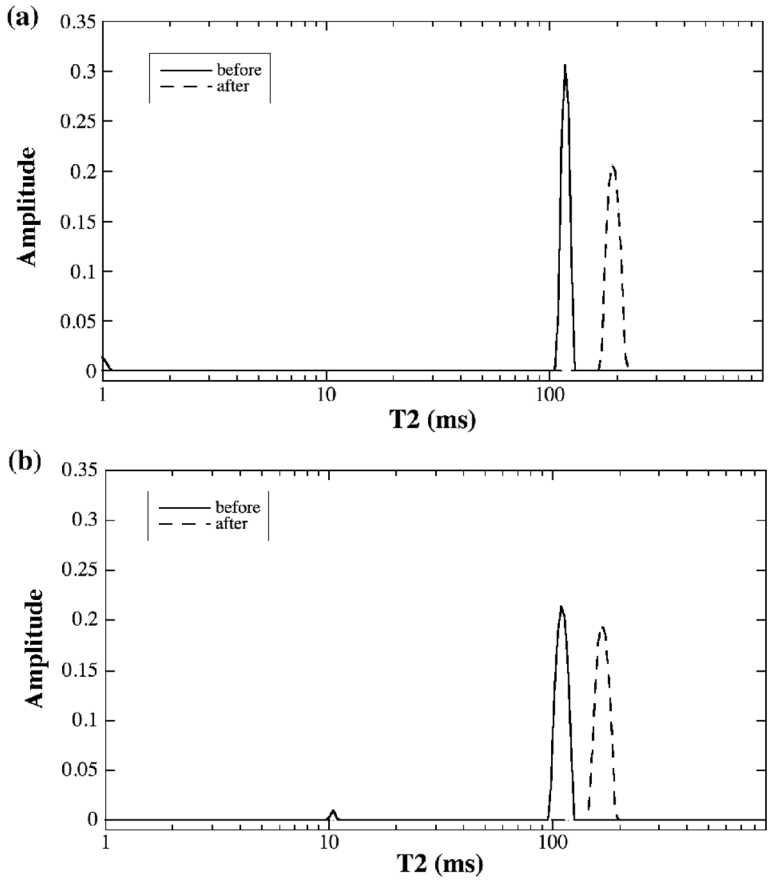

Fig 3.

The T_2 distribution plots from the data shown in Fig 2, (a) T_2 from NMR spectroscopy and (b) T_2 from μMRI. Apart from occasional minor peaks that are less than 3% of the total population, T_2 in bovine nasal cartilage has only one component.

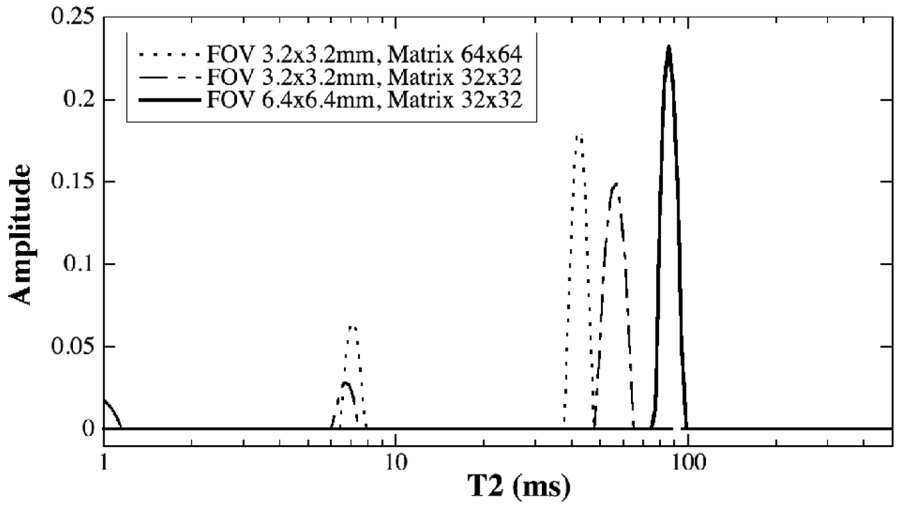

Fig 4.

The plots of T_2 distribution from the same BNC sample by μMRI with the standard MSME sequence. For FOV at both 6.4×6.4 mm^2 (solid line) and 12.8×12.8 mm^2 (not shown), T_2 has only one component. When FOV is reduced to 3.2×3.2 mm^2 (whether the data matrix was 32×32 or 64×64), T_2 becomes two components.

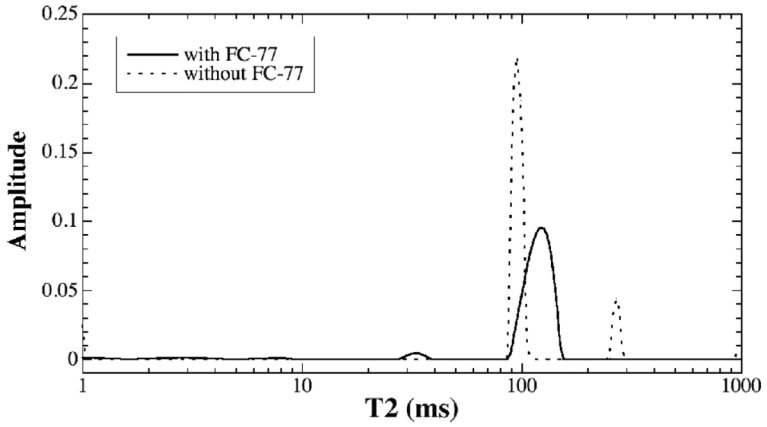

Fig 5.

The influence of the magnetic susceptibility on the multi-component T_2 measurement in a 5-mm-long BNC: the specimen immersed in FC-77 liquid vs. exposed in air.

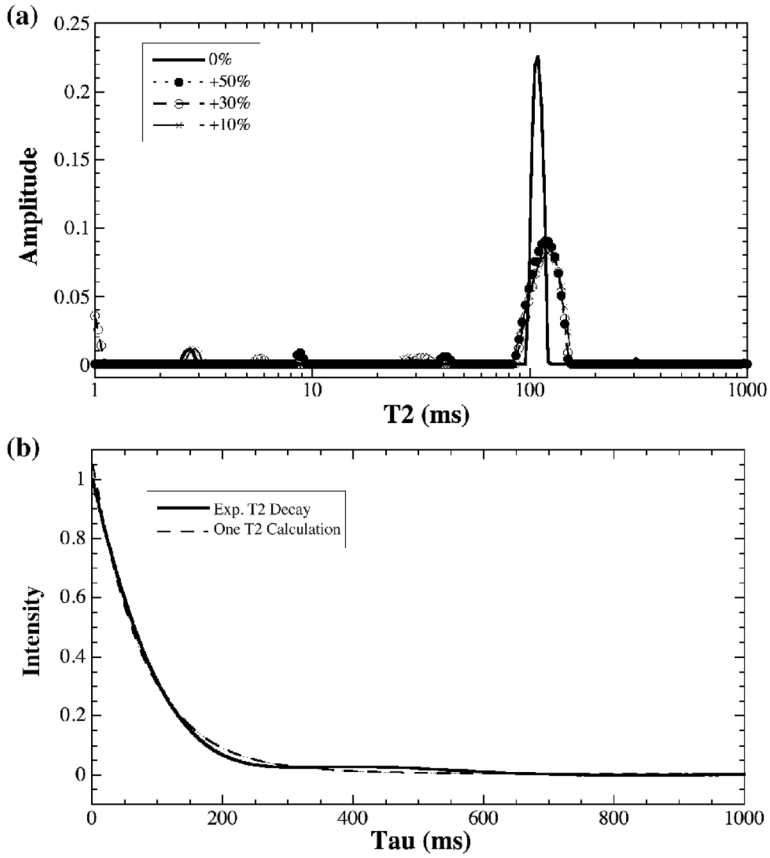

Fig 6.

The influence of (a) the 90°imperfection by changing the 90° pulse duration by up to 50%, and (b) the magnetic field inhomogeneity by worsening the line width by up to 4 times or by using a 1-mm-long sample without immersed in the FC-77 liquid. Either a single or multiple exponential decays could not fit this set of distorted data. A single T_2 decay is plotted in (b) as a comparison.

Table 1

Simulation data in Admissibility Test

Simulation Parameters		$T_2$1 (ms)	W_1 (%)	$T_2$2 (ms)	W_2 (%)	$T_2$3 (ms)	W_3 (%)
3 Components		2.5	10	25	20	95	70
2 Components		5	50	45	50		
1 Component	**Test 1**	5	100				
	Test 2	50	100				
	Test 3	150	100				

Table 2

Summary of multi-component T2 data in bovine nasal cartilage

	Spectroscopy	Imaging				
Sequence	**CPMG**	**CPMG-SE**	**MSME**			
	T_2 (ms)	**T_2 (ms)**	**$T_2$1 (ms)**	**W_1 (%)**	**$T_2$2 (ms)**	**W_2 (%)**
Before Trypsin	113.5±3.9	113.2±4.0	7.9±2.3	16.7±7.0	40.7±0.8	83.3±7.0
After Trypsin	167.0±23.0	175.2±2.3	6.8±0.9	23.7±7.0	41.2±0.8	76.3±7.0